Proceedings of the
8th Graz Brain-Computer Interface Conference 2019 DOI: 10.3217/978-3-85125-682-6-19

SIMULTANEOUS DECODING OF VELOCITY AND SPEED DURING EXECUTED AND OBSERVED TRACKING MOVEMENTS: AN MEG STUDY

R.J. Kobler[1,2], M. Hirata[2,3], H. Hashimoto[2,3], R. Dowaki[2,4], A.I. Sburlea[1], G.R. Müller-Putz[1]

[1]Institute of Neural Engineering, Graz University of Technology, Graz, Austria
[2]Endowed Research Department of Clinical Neuroengineering, Osaka University, Suita, Japan
[3]Department of Neurosurgery, Osaka University Graduate School of Medicine, Suita, Japan
[4]Hiroshima University School of Medicine, Hiroshima, Japan

E-mail: mhirata@nsurg.med.osaka-u.ac.jp, {reinmar.kobler, gernot.mueller}@tugraz.at

ABSTRACT: Brain signals carry rich information about voluntary upper-limb movements. Accessing this information to control an end-effector (upper-limb, robotic arm, cursor) has been a central topic in brain-computer interface (BCI) research. To date, non-invasive BCIs based on kinematics decoding have focused on extracting partial information (i.e, single or highly correlated kinematic parameters). In this work, we show that low-frequency magnetoencephalographic (MEG) signals simultaneously carry information about multiple kinematic parameters. Using linear models, we decoded cursor velocity and speed during executed and observed tracking movements with moderate (0.2 to 0.4) correlation coefficients (CCs). Comparing the CCs between executed and observed tracking movements, revealed that the MEG signals carried more information (0.1 higher CCs) about velocity and speed during the executed tracking movements. The higher correlations were mainly explained by increased predictive activity in primary sensorimotor areas. We could, therefore, show that non-invasive BCIs have the potential to extract multiple kinematic signals from brain activity in sensorimotor areas.

INTRODUCTION

Decoding voluntary movement from electrophysiological brain signals has been a central topic in brain-computer interface (BCI) research. In recent years, invasive approaches have demonstrated that individuals who lost control of their upper-limb could successfully control a robotic arm [1] or even regain control of their upper-limb [2]. These invasive BCI systems typically decode various movement parameters from spiking rates of neurons in primary sensorimotor areas [3, 4]. It has long been assumed that non-invasive functional neuroimaging techniques such as electroencephalography (EEG) and magnetoencephalography (MEG) lack the spatial resolution to decode the kinematics of voluntary movements. However, it has been shown otherwise by various studies in the past decade [5–7]. However, the predicted end-effector position of non-invasive decoders typically has a lower signal to noise ratio (SNR) compared to the invasive decoders. We think that the combined decoding of multiple kinematic signals could improve the SNR and, thereby, elevate the performance of non-invasive decoders.

A myriad of non-invasive studies in this field of BCI research has investigated either directional (e.g, velocity, position) or non-directional (e.g, speed) kinematic signals in isolation [6, 8–10]. Bradberry et al. were the first to show that low-frequency EEG signals carried information about positions and velocities during reaching movements [11]. Complementary, Waldert et al. showed that reach direction can be classified from low-frequency EEG and MEG [12]. Jerbi et al. showed that low-frequency MEG signals are coupled to hand speed during a continuous visuomotor (VM) task [8]. Recent invasive studies using Electrocorticographic (ECoG) signals demonstrated that velocity and speed can be decoded simultaneously from low-frequency brain signals in primary sensorimotor areas [13, 14]. Taken together, we surmise that velocity and speed can be jointly decoded from non-invasive M/EEG signals.

We believe that a pursuit tracking task (PTT) is ideally suited to investigate this question. A PTT is characterized by two stimuli - a traget stimulus moving along random trajectories and an end-effector (e.g., cursor). The end-effector is used to track the target stimulus. The PTT has two favorable properties. First, the kinematics vary continuously in a frequency range that can be controlled by the experimenter. Second, the target trajectories can be designed so that specific kinematic signals are jointly uncorrelated. Using a PTT, we showed that the low-frequency EEG originating in premotor and primary sensorimotor areas was preferentially tuned to cursor velocity rather than cursor position [15].

In this study, we investigated the joint decoding of cursor velocity and speed from low-frequency MEG activity during a two-dimensional PTT. Our paradigm separated two conditions. In the first condition (execution), participants tracked the target with their gaze and a cursor. In the second condition (observation), participants tracked the target only with their gaze. This allowed us to address two questions. First, can velocity and speed be decoded simultaneously from non-invasively acquired brain activity during voluntary upper-limb movements? Second, does the decoding performance change if the upper-limb is not involved in the tracking task?

 DOI: 10.3217/978-3-85125-682-6-19

MATERIALS AND METHODS

23 healthy people participated in this study. 5 were female and 18 male. They were 28.5 ± 2.4 (standard-error of the mean; sem) years old, had normal or corrected to normal vision, and self-reported to be right-handed. The experimental procedure conformed to the declaration of Helsinki and was approved by the ethics committee of the Osaka University hospital. We could not complete the experiment for three participants and identified that one participant was positioned incorrectly inside the MEG scanner during the offline analysis. These four participants were excluded from the final offline analysis.

Figure 1a depicts the experimental setup. The participants were lying in a supine position, with the head resting on a cushion inside an MEG scanner. A projection screen fixed in front of their face presented visual stimuli. We used two visual stimuli, a target and a cursor. The cursor could be controlled by the participants through moving their right hand's index finger on a 2D surface. The tip of the index finger was tracked with a custom optical motion capture system.

After each participant found a comfortable position for his/her right arm and hand, the position of the marker was defined as the resting position. The resting position was mapped to the center of the screen. Finger movements, within a 1.5 centimeter radius around the resting position were mapped to cursor movements within a circle confined by the bounds of a virtual grid. Rightward/forward finger movements were mapped to rightward/upward cursor movements.

As in our previous study [15], the experimental procedure consisted of 4 blocks, lasting for about 3 hours in total. In the first block (10 minutes), the participants could familiarize themselves with the paradigm. In the second block, we recorded eye artifacts and resting activity as described in [16] for about 12 minutes (2 runs; each 6 minutes). During the third block, the main experimental task was performed. The fourth block at the end of the experiment was identical to the second one.

Figure 1b outlines the paradigm of the main experimental task. We investigated a PTT in two conditions. A yellow target stimulus indicated the beginning of a new trial. After 2 s of preparation, the target changed its color to green (execution condition) or blue (observation condition).

In the execution condition, the participants were asked to track the target with their gaze and the cursor. In the first experimental block, each participant trained to minimize the distance to the target and to make smooth cursor movements.

In the observation condition, the participants would only track the target with their gaze and keep their finger in the resting position. In order to achieve similar visual input and tracking dynamics in both conditions, we replayed matching cursor trajectories.

The target moved along pseudo-random trajectories, which were generated from pink noise in the [0.3, 0.6] Hz band. The horizontal and vertical components of the target trajectories were independent and identically distributed. This required the participant to control the cursor in 2 dimensions at the same time. The detailed target trajectory generation and cursor trajectory replay procedures are presented in [15].

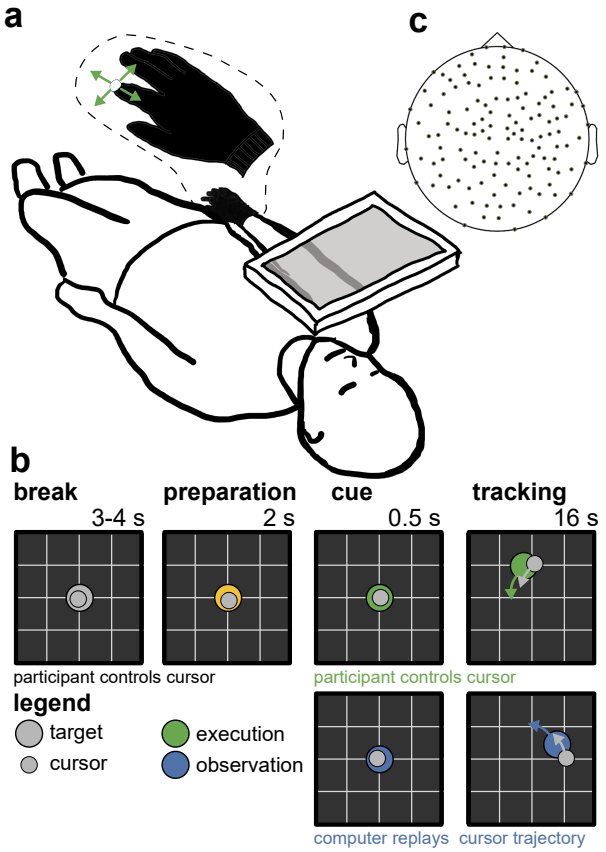

Figure 1: Overview of the experiment. **a**, Experimental setup. The participants were lying in a supine position inside an MEG scanner. They moved their right index finger on a 2D surface to control a cursor on the screen. **b**, Experimental paradigm. Each trial started with a 2 s preparation period. The participants were asked to keep the cursor in the center (i.e, the right index finger in the resting position). After a condition cue, the target stimulus moved along a pseudo-random trajectory for 16 s. In the execution condition (green), the participants tracked the target with both their gaze and the cursor. In the observation condition, they tracked the target only with their gaze. **c**, Topographic distribution of the 129 MEG sensors used in this study.

The paradigm consisted of 160 trials (80 per condition; pseudo-randomly distributed). They were presented in 10 runs (6 minutes each). In between runs, participants could rest for about 2 to 3 minutes. During the experiment, we tested if the finger was in the resting position during the preparation (both conditions) and tracking periods (observation condition). If the position exceeded a threshold, a trial was aborted. On average, 5.2 trials were aborted, resulting in 154.8 complete trials.

Neuromagnetic activity was recorded with a 160 channel whole-head MEG system (MEGvision NEO, Yokogawa Electrip Corp., Kanazawa, Japan) housed in a magnetically shielded room. For this study, we used the signals of 129 sensors (Figure 1c). Electrooculographic (EOG) signals were recorded with 4 electrodes placed at the outer canthi (horizontal EOG) and above/below the left eye

 DOI: 10.3217/978-3-85125-682-6-19

(vertical EOG). The EOG signals were recorded with a 128-channel EEG system (Neurofax EEG 1200, Nihon Koden Corp., Tokyo, Japan). MEG and EOG signals were recorded synchronously at rate a of 1 kHz.

We asked participants to keep their head and shoulder position fixed during the experiment (blocks 2 to 4). We additionally monitored the head position inside the MEG system with five marker coils, attached to the face. Their position was measured at the beginning of each run.

The custom motion capture and visual stimuli signals were recorded at 60 Hz using the labstreaminglayer (LSL) protocol[1]. We implemented the paradigm in Python 2.7 based on the simulation and neuroscience application (SNAP) platform[2]. Using pilot experiments, we determined the delay between the finger and the cursor movement on the screen. The delays introduced by the hard- and software added up to 190 ms.

We analyzed the recorded data offline with a custom-made pipeline that we implemented with Matlab (Matlab 2015b, Mathworks Inc., USA) and the open source toolboxes EEGLAB [17] (version 14.1.1) and Brainstorm [18] (version 05-Jun-2018). We first synchronized the stimuli and MEG signals by aligning impulses captured by a photodiode. After synchronization, all signals were resampled to 200 Hz. We estimated the cursor velocities by applying a Savitzky-Golay finite impulse response (FIR) differentiation filter (polynomial order 3, 21 filter taps, zero-phase) to the cursor positions.

To compensate small head movements across runs, we spherically interpolated the MEG sensors of all runs (10 tracking, 4 eye) to their average position in relation to the participant's head. If the maximal distance of any channel to the average position was larger than 25 mm, the run was discarded. We discarded 2 runs in total. The grand-average maximal channel distance across accepted runs was 5±0.1 mm (sem). After merging the signals of the tracking runs, we applied high-pass (0.25 Hz cut-off frequency, Butterworth filter, eight order, zero-phase) and band-stop (59 and 61 Hz cut-off frequencies, Butterworth filter, fourth order, zero-phase) filters. To compensate technical and spatially stationary artifacts introduced by equipment, we applied independent component analysis (ICA). In detail, we applied the extended infomax algorithm to decompose the MEG signals (high-pass filter with 0.4 Hz cut-off frequency) into independent components (ICs) that explained 99.9 % of the variance. We visually inspected and marked 8.6±0.2(sem) of 63.5±0.1(sem) ICs for rejection. They were then removed from the 0.25 Hz high-pass filtered signals. We attenuated eye movement and blink artifacts by applying the artifact subspace subtraction algorithm [15, 16]. To extract the low-frequency MEG signals, we applied a low-pass filter to the broadband MEG signals (2 Hz cut-off frequency, Butterworth filter, sixth order, zero-phase) and resampled all signals at 10 Hz.

We then epoched the continuous data into 14 s trials, starting 1.5 s after the condition cue. Trials were marked for rejection, if (1) the broadband MEG signal of any sensor exceeded a threshold (±5 fT), (2) had a abnormal probability, variance or kurtosis (≥ (6/4/6) standard-deviations (stds) beyond the mean), (3) the correlation between the EOG and the target position signals were improbable (≥ 4 stds beyond the mean), or (4) a tracking error happened (i.e., jerky or no cursor movement). All criteria combined resulted in rejecting 26.6±0.4(sem) of 154.8 trials.

Cursor velocity and speed were estimated with a sliding-window, linear regression approach [11, 15, 19]. At single lags, a partial least-squares (PLS) estimator was used to decode a single kinematic signal (horizontal velocity, vertical velocity or speed) from the pre-processed MEG signals. Similar to [15], the PLS estimator considered 10 latent components. The model was evaluated using a 10 times 5 fold cross-validation (CV) scheme with the evaluation metric being Pearson correlation coefficients (CCs) between the recorded kinematic signals and their neural estimates. We estimated chance level performance by shuffling the kinematic signals across trials of the same condition. We then applied 5 fold CV to the shuffled data and repeated the shuffling and CV evaluation 1000 times.

The weights of the linear regression model can be readily transformed to patterns [20]. We computed scaled patterns according to [15].

To ease neurophysiological interpretation, we projected the scaled patterns to the cortical surface of the ICBM152 template boundary element (BEM) head model [21]. We co-registered the template with the head of each participant (and the MEG sensors) by manually fitting the template head model to digitized head points (50 to 60 points per participant) in Brainstorm toolbox. OpenMEEG [22] was applied to compute the forward model for 5011 voxels on the cortical surface. sLORETA [23] was used to estimate the inverse solution for unconstrained sources at the 5011 voxels. The noise covariance matrix was estimated using 5 minutes of resting data (similar preprocessing as the tracking data), recorded during experimental blocks 2 and 4, and applying shrinkage regularization (10% of its largest eigenvalue).

RESULTS

Grand-average results presented here are summarized by the mean and its standard-error across the 19 participants.

We assessed the participants tracking behavior by computing CCs between the target and cursor position signals in the execution condition. The CCs peaked at 0.22±0.01 s for the horizontal component and 0.23±0.01 for the vertical component. That is, the target signal lead the cursor by approximately 225 ms on average. The CCs at the peaks were 0.90±0.01 (horz) and 0.92±0.01 (vert).

We also assessed the visual tracking behavior in both conditions by computing CCs between the horizontal/vertical target position and horizontal/vertical EOG signals. In the execution condition, the CCs were 0.94±0.01 (horz) and 0.79±0.06 (vert). In the observation condition, they

[1] https://github.com/sccn/labstreaminglayer
[2] https://github.com/sccn/SNAP

 DOI: 10.3217/978-3-85125-682-6-19

were 0.92±0.01 (horz) 0.70±0.06 (vert).

The auto-/cross-correlation curves in Figures 2a-c demonstrate that during the PTT the three signals of interest (horizontal/vertical cursor velocity and cursor speed) were negligibly correlated. The grand-average cross-correlations were below or equal to 0.1 in both conditions. Similar auto-/cross-correlation curves in both conditions show that the cursor trajectories in observation condition (dashed lines) were similar to the executed ones (solid lines).

Figures 2d-f show the grand-average CV test-set CCs between the decoded and recorded kinematic signals for single-lag, sliding-window, linear regression models. We decoded the cursor velocities and speed from the MEG signals of all 129 sensors at lags ranging from [-0.5, 0.5] s in steps of 0.1 s. The MEG sensor signals lead the cursor signals for negative lags.

We used the CCs of the shuffled data to test if the observed results were due to chance. We controlled the false-discovery rate (FDR) at a significance level $\alpha = 0.05$ for $n_{comparisons} = n_{metrics} \cdot n_{lags} = 3 \cdot 11 = 33$ comparisons per subject [24]. The tables at the bottom of Figures 2d-f list the results.

The horizontal cursor velocity decoding results are summarized in Figure 2d. The decoding model performed above chance level for all lags and participants in the execution condition and almost all participants in the observation condition. The execution condition CCs were larger than the observation condition ones for all lags. The paired difference between conditions (exe-obs) peaked at lag -0.3 s.

The vertical cursor velocity decoding results are summarized in Figure 2e. The CCs were above chance level for all lags and participants. Compared to the horizontal velocity results, we observed higher CCs in the execution condition and similar CCs in the observation condition. As a consequence, the paired difference was higher (peaked at lag -0.1 s).

The cursor speed decoding results are displayed in Figure 2f. All CCs were above chance level in the execution condition. In the observation condition, the results varied across lags and ranged from 14 to 18 participants having CCs above chance level. Compared to the velocities, the CCs were lower by approx. 0.1 in both conditions. However, the effect size of condition was comparable to the velocities (paired difference peak of 0.15 at lag -0.3 s).

To identify the spatiotemporal encoding of information about cursor velocities and speed, we transformed the model weights to patterns at the cortical surface. Figures 2g-i show the grand-average patterns at selected lags for execution condition (top), observation condition (middle) and the paired-difference (bottom). The paired-differences for all three kinematic signals show that the predictive pattern activity in contra-lateral primary-sensorimotor (SM1) areas was larger in execution condition at negative lags. Thus, contra-lateral SM1 activity carried information about the upcoming cursor velocities and speed in the execution condition. The difference was maximal at lags -0.3 to -0.2 s and varied across the signals of interest (speed > vertical velocity > horizontal velocity).

We also observed that superior parietal and parieto-occipital areas carried predictive information about the three kinematic signals in both conditions (Figures 2g,h top and middle row). The paired-differences indicate that the activity in these areas was similarly predictive for horizontal cursor velocity in both conditions (Figure 2g), more predictive for vertical cursor velocity in execution condition (Figure 2h), and less predictive for cursor speed in execution condition (Figure 2i).

DISCUSSION

We have demonstrated simultaneous decoding of cursor velocity and speed information by means of low-frequency MEG signals during a PTT. The PTT allowed us to study continuous, uncorrelated cursor velocity and speed signals (Figures 2a-c). During executed index finger tracking movements, contra-lateral SM1 activity was simultaneously predictive for cursor velocity and speed, while superior parietal and parieto-occipital activity was also predictive in observed tracking movements.

Linear, single-lag decoding model performance in terms of CCs was above chance level for all participants during execution condition, and almost all participants during observation condition (Figures 2d-f). The range of CCs is in agreement with the results of previous linear M/EEG kinematics decoding studies [11, 15, 25].

Comparing the two conditions, we found that the MEG signals contained more information about the cursor velocities and speed in the execution condition (Figures 2d-f). The average effect of condition was stronger for the vertical cursor velocity than for the horizontal one. This is in accordance with the findings of our previous EEG study [15].

The differences in the decoder patterns (Figures 2g-i; bottom row) indicate that the activity in contra-lateral SM1 carried more information about the uncorrelated velocity and speed signals in the execution condition. The differences peaked at lags -0.3 s (horizontal cursor velocity; Figure 2,g), -0.2 s (vertical cursor velocity; Figure 2,h) and -0.3 s (cursor speed; Figure 2,i) respectively. Since the difference in decoder CCs in Figures 2d-f were modulated by these peaks, the activity in contra-lateral SM1 must have considerably contributed to the larger decoder CCs in the execution condition.

Considered that the cursor movement was the 190 ms delayed index finger movement, the observed peaks are plausible in terms of neurophysiology [26]. Simultaneous decoding of velocity and speed from contra-lateral SM1 has also been demonstrated by recent invasive studies based on spiking activity [27] and low-frequency ECoG signals [14]. Inoue et al. observed that the firing rates of a large fraction of neurons in SM1 were simultaneously tuned to speed and velocity [27]. Hammer et al. reported a stronger encoding of end-effector speed compared to velocity in low-frequency ECoG signals [14]. This in

 DOI: 10.3217/978-3-85125-682-6-19

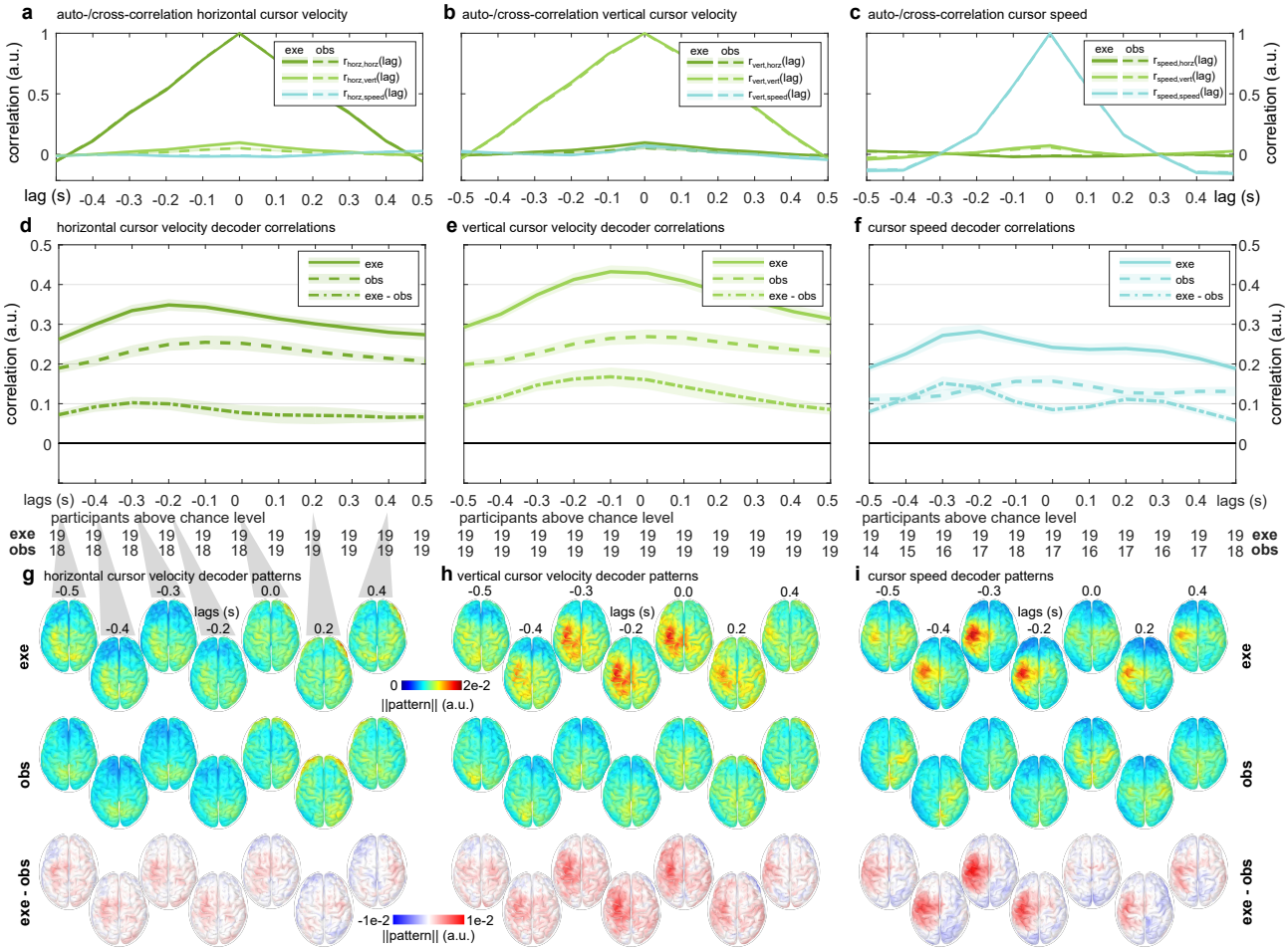

Figure 2: Grand-average results of the experiment. Shaded areas indicate the sem across the 19 participants. **a**, Auto-/cross-correlation curves for the three metrics of interest relative to the horizontal cursor velocity. **b,c**, As in **a** for the vertical cursor velocity (**b**) and cursor speed (**c**). **d**, CV Test-set correlations between the recorded horizontal cursor velocity and its decoded estimate for execution condition (solid line), observation condition (dashed line) and their paired difference (dash-dotted line). MEG sensor signals lead the horizontal cursor velocity signal for negative lags. The table below lists the number of participants whose single-lag decoder CCs were above chance level. **e,f**, As in **d** for the vertical cursor velocity (**e**) and cursor speed (**f**). **g**, Horizontal cursor velocity decoder patterns for selected lags. We projected the patterns to voxels of a template BEM head model and averaged their norms across participants. **h,i**, As in **g** for the vertical cursor velocity (**h**) and cursor speed (**i**).

agreement with our results. I.e, in execution condition, the speed decoder patterns in SM1 were larger than the velocity decoder patterns.

The decoder patterns (Figures 2g-i; top and middle rows) showed also common activity in execution and observation condition. In both conditions, superior parietal and parieto-occipital areas were predictive. Their activation in both conditions is in agreement with findings of our previous study [15] and also fMRI studies on executed and observed reaching movements [28, 29].

CONCLUSION AND FUTURE WORK

In this work we have shown that non-invasive MEG signals simultaneously carry information about velocity and speed of executed and observed tracking movements. Linear, single-lag decoders extracted more information originating in contra-lateral SM1 during executed tracking movements. Whereas superior parietal and parito-occipital areas were informative in executed and observed tracking movements.

Despite the encouraging results presented here, further research is imperative. It needs to be shown that a combined decoding of velocity and speed indeed improves the SNR of the predicted end-points offline and subsequently online. Moreover, studies with humans who lost control of their upper-limb will have to demonstrate whether non-invasive, decoding of imagined body kinematics has the potential to improve their quality of life.

ACKNOWLEDGEMENTS

The authors acknowledge Catarina Lopes Dias, Joana Pereira and Lea Hehenberger for their valuable comments. This work has received funding from the European Research Council (ERC) via the consolidator grant 681231 ‘Feel Your Reach’, from Graz University of Technology via its short-time research abroad scholarship, from the Japan Society for the Promotion of Science (JSPS) program KAKENHI (26282165), from the National Institute of Information and Communications Technology (NICT), from the Council for Science, Tech-

nology and Innovation (Cabinet Office, Government of Japan) program ImPACT, and from a research grant form the Ministry of Internal Affairs (Government of Japan).

REFERENCES

[1] Collinger JL, Wodlinger B, Downey JE, *et al.* High-performance neuroprosthetic control by an individual with tetraplegia. The Lancet. 2013;381(9866):557–564.
[2] Ajiboye AB, Willett FR, Young DR, *et al.* Restoration of reaching and grasping movements through brain-controlled muscle stimulation in a person with tetraplegia: A proof-of-concept demonstration. The Lancet. 2017;389(10081):1821–1830.
[3] Lebedev MA, Nicolelis MAL. Brain-Machine Interfaces: From Basic Science to Neuroprostheses and Neurorehabilitation. Physiological Reviews. 2017;97(2):767–837.
[4] Branco MP, Boer LM de, Ramsey NF, *et al.* Encoding of kinetic and kinematic movement parameters in the sensorimotor cortex: A brain-computer interface perspective. European Journal of Neuroscience. 2019.
[5] Jerbi K, Vidal JR, Mattout J, *et al.* Inferring hand movement kinematics from MEG, EEG and intracranial EEG: From brain-machine interfaces to motor rehabilitation. Irbm. 2011;32(1):8–18.
[6] Robinson N, Vinod AP. Noninvasive Brain–Computer Interface: Decoding Arm Movement Kinematics and Motor Control. IEEE Systems, Man, & Cybernetics Magazine. 2016;2(October):4–16.
[7] Fukuma R, Yanagisawa T, Saitoh Y, *et al.* Real-time control of a neuroprosthetic hand by magnetoencephalographic signals from paralysed patients. Scientific Reports. 2016;6(1):21781.
[8] Jerbi K, Lachaux JP, N'Diaye K, *et al.* Coherent neural representation of hand speed in humans revealed by MEG imaging. PNAS. 2007;104(18):7676–7681.
[9] Bourguignon M, Jousmäki V, Op de Beeck M, *et al.* Neuronal network coherent with hand kinematics during fast repetitive hand movements. NeuroImage. 2012;59(2):1684–1691.
[10] Marty B, Bourguignon M, Jousmäki V, *et al.* Cortical kinematic processing of executed and observed goal-directed hand actions. NeuroImage. 2015;119:221–228.
[11] Bradberry TJ, Gentili RJ, Contreras-Vidal JL. Reconstructing Three-Dimensional Hand Movements from Noninvasive Electroencephalographic Signals. Journal of Neuroscience. 2010;30(9):3432–3437.
[12] Waldert S, Preissl H, Demandt E, *et al.* Hand movement direction decoded from MEG and EEG. Journal of Neuroscience. 2008;28(4):1000–1008.
[13] Bundy DT, Pahwa M, Szrama N, *et al.* Decoding three-dimensional reaching movements using electrocorticographic signals in humans. Journal of neural engineering. 2016;13(2):026021.
[14] Hammer J, Pistohl T, Fischer J, *et al.* Predominance of Movement Speed over Direction in Neuronal Population Signals of Motor Cortex: Intracranial EEG Data and A Simple Explanatory Model. Cerebral Cortex. 2016;26(6):2863–2881.
[15] Kobler RJ, Sburlea AI, Müller-Putz GR. Tuning characteristics of low-frequency EEG to positions and velocities in visuomotor and oculomotor tracking tasks. Scientific Reports. 2018;8(1):17713.
[16] Kobler RJ, Sburlea AI, Müller-Putz GR. A comparison of ocular artifact removal methods for block design based electroencephalography experiments. In: Proc. of the 7th Graz BCI Conference. 2017, 236–241.
[17] Delorme A, Makeig S. EEGLAB: An open source toolbox for analysis of single-trial EEG dynamics including independent component analysis. Journal of Neuroscience Methods. 2004;134(1):9–21.
[18] Tadel F, Baillet S, Mosher JC, *et al.* Brainstorm: A user-friendly application for MEG/EEG analysis. Computational Intelligence and Neuroscience. 2011;2011:8.
[19] Ofner P, Müller-Putz GR. Using a noninvasive decoding method to classify rhythmic movement imaginations of the arm in two planes. IEEE Trans. Bio. Eng.. 2015;62(3):972–981.
[20] Haufe S, Meinecke F, Görgen K, *et al.* On the interpretation of weight vectors of linear models in multivariate neuroimaging. NeuroImage. 2014;87:96–110.
[21] Fonov V, Evans AC, Botteron K, *et al.* Unbiased average age-appropriate atlases for pediatric studies. NeuroImage. 2011;54(1):313–327.
[22] Gramfort A, Papadopoulo T, Olivi E, *et al.* OpenMEEG: Opensource software for quasistatic bioelectromagnetics. BioMedical Engineering Online. 2010;9.
[23] Pascual-Marqui RD. Standardized low resolution brain electromagnetic tomography (sLORETA): technical details. Methods & Findings in Experimental & Clinical Pharmacology. 2002;24:1–16.
[24] Benjamini Y, Hochberg Y. Controlling the false discovery rate: a practical and powerful approach to multiple testing. J. Royal Stat. Soc. B. 1995;57(1):289–300.
[25] Bradberry TJ, Rong F, Contreras-Vidal JL. Decoding center-out hand velocity from MEG signals during visuomotor adaptation. NeuroImage. 2009;47(4):1691–1700.
[26] Miall RC, Wolpert DM. Forward models for physiological motor control. Neural Networks. 1996;9(8):1265–1279.
[27] Inoue Y, Mao H, Suway SB, *et al.* Decoding arm speed during reaching. Nature Communications. 2018;9(1):5243.
[28] Filimon F, Nelson JD, Huang RS, *et al.* Multiple Parietal Reach Regions in Humans: Cortical Representations for Visual and Proprioceptive Feedback during On-Line Reaching. Journal of Neuroscience. 2009;29(9):2961–2971.
[29] Magri C, Fabbri S, Caramazza A, *et al.* Directional tuning for eye and arm movements in overlapping regions in human posterior parietal cortex. NeuroImage. 2019;(in press).